High-Density, Aligned SiO_2 Nanowire Arrays: Microscopic Imaging of the Unique Growth Style and Their Ultraviolet Light Emission Properties

Zhidong Xiao,* Lide Zhang,* Guowen Meng, Xike Tian, Haibo Zeng, and Ming Fang

Key Laboratory of Materials Physics, Institute of Solid State Physics, Chinese Academy of Sciences, Hefei, 230031 P. R. China

Received: April 10, 2006; In Final Form: June 28, 2006

High-density, free-standing SiO_2 nanowire arrays were successfully fabricated by a simple chemical vapor deposition method through a controlled pattern of the micrometer-sized alloyed balls on the Si substrate combined with a local balanced and steady-state reaction vapor environment. The direct observation of temporal evolution of the SiO_2 nanowire growth process via the microscopic imaging approach offers us amazing pictures related to the unique vapor−liquid−solid (VLS) growth styles. These novel results are beneficial to understanding the formation mechanism of silica nanowire arrays, and at the same time, they extend our knowledge of VLS growth phenomena. The stable and strong ultraviolet emission properties of the as-grown products are of significant interest for their potential applications related to nanoscale optoelectronic device including ultraviolet-light-emitting devices, etc.

1. Introduction

The fabrication of one-dimensional (1D) nanostructures has attracted a great deal of interest in nanotechnology recently because they have remarkable physical properties and fascinating geometries and have great potential for nanoscale electronics and optoelectronics.[1−16] In particular, 1D silicon oxide nanomaterials are good candidates for photoluminescent, biocompatible materials, and their surfaces are accessible to be modified specifically. Therefore, they can often find applications in the areas of nanoscale electronic devices, catalysis, and the protection of environmentally sensitive materials etc.[17−19]

To date, several methods have been applied to produce silicon oxide nanowires, including laser ablation, sol−gel, carbonthermal reduction, and chemical vapor deposition (CVD).[20−24] However, these previous reports only produced undesirably sparsely populated, randomly oriented silicon oxides nanowires, resulting in difficulties in direct integration of the nanowires into the nanoscale devices. Especially, extended and highly oriented nanowire arrays will definitely possess outstanding collective behaviors,[25] which will make them promising for many applications, including microelectronic devices, chemical and biological sensing, light-emitting displays, catalysis, drug delivery, separation, and optical storage, etc. To our best knowledge, the direct fabrication of highly oriented, large-scale of silicon oxide nanowire arrays with a controlled morphology still remains a significant challenge. On the other hand, it is vital to elucidate the underlying growth mechanisms that determine the morphology and dimensionality of the 1D nanostructure arrays. Specifically, despite over 40 years of investigations, many characteristics of the well-known vapor−liquid−solid (VLS) growth[26] are still not well understood. For example, in the conventional picture of the VLS growth, the prevalent views assume that each of the catalyst alloyed particles will keep the fixed morphology and direct just one piece of nanowire growth during the whole growth process. There also exist claims that larger alloyed catalyst particles are generally unfavorable for the relevant catalyzed growth of nanowires owning to their shape fluctuations.[27] Through microscopic imaging the specific VLS growth process in our protocol, one might gain some new insight into better understanding of nanowire growth mechanism as well as better controlling the formation of nanowire array.

Herein, we report using a modified simple chemical vapor deposition method to synthesize high-density, free-standing silicon oxide nanowire arrays. In addition, we conducted a series of time-dependent microscopic imaging experiments designed to elucidate the fascinating aspects of the current specific VLS growth process. Furthermore, the as-synthesized products exhibit remarkable ultraviolet light-emission properties under optical excitation. So, these nanowire arrays might be envisaged to find various applications such as optical sensing and optical communication etc.

Recently, Lee's group has systematically explored the growth of well-aligned ZnO nanowire arrays on silicon substrate via a simple horizontal double-tube system.[28] Inspired by their successes, we expand this synthetic procedure to control the growth of desired high-density, aligned SiO_2 nanowire arrays under a fairly less stringent condition, which successfully guarantees the growth process to take place in a local balanced and steady-state vapor environment. In addition, unlike conventional VLS method for the growth of nanowires, one of the precursors (Si) in our protocol comes from the Si substrate.

2. Experimental Section

Fabrication of the Silicon Oxide Nanowire Arrays. The double-tube system experimental setup is similar to that formerly used for the synthesis of ZnO nanowire arrays,[28] as shown in Scheme 1. Briefly, a big horizontal ceramic tube (inner diameter 45 mm, length 150 cm) was mounted inside a tube furnace, then a smaller ceramic tube with one end sealed (inner diameter 18 mm, length 60 cm) was inserted into the above-mentioned big tube. An alumina boat containing a mixture of carbon black

* To whom correspondence should be addressed. E-mail (Z.X.): zdxiao@issp.ac.cn.

10.1021/jp0622233 CCC: $33.50
Published on Web 07/27/2006

SCHEME 1: Experimental Setup Used for the Synthesis of SiO_2 Nanowire Array

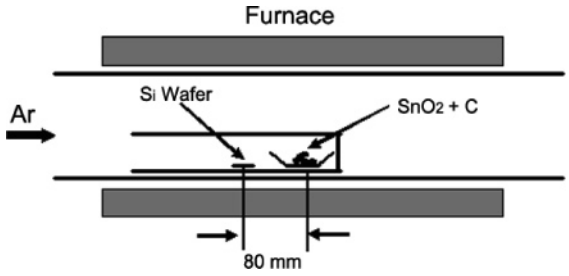

(97 wt % purity, 0.3 g), SnO_2 (0.2 g) was loaded into the closed end of the small tube, which corresponds to the center region of the bigger ceramic tube. A precleaned silicon wafer was placed at the open end of the smaller tube with a distance of 8 cm from the source materials. After the tube had been purged with high-purity Ar for 30 min, the temperature at the central region of the furnace was increased to 1150 °C in 10 min and kept at this temperature for 30 min in flowing Ar gas (60 sccm). The temperature at the substrate was close to 500 °C, as determined from the premeasured temperature gradient curve. After the furnace had cooled to room temperature, a white wool-like product was deposited on the Si substrate.

Characterization. The collected samples were characterized by FEI field emission scanning electron microscopy (FE-SEM, FEI Sirion 200) with an EDX facility, HR-TEM (JEOL 2010, operated at 200 KV), and also an EDX attached to the HRTEM. The emission spectrum was recorded with an Edingburgh luminescence spectrometer (FLS 920) using a xeron lamp (900) as excitation source at room temperature.

3. Results and Discussion

FE-SEM was employed to characterize the geometric configuration of the as-synthesized product. Shown in Figure 1a,b

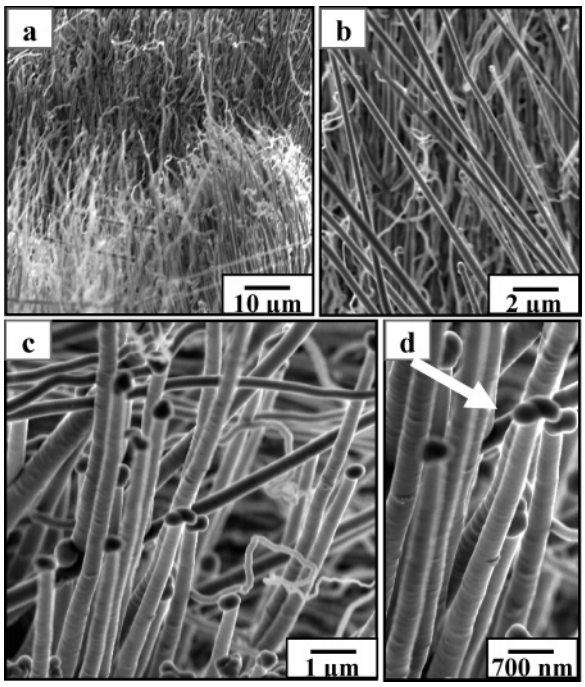

Figure 1. SEM images of high-density arrays of free-standing SiO_2 nanowires: (a, b) low-magnification cross-section SEM images; (c, d) high-magnification images of the as-grown nanowires, revealing the irregular tip shapes (indicated with arrow in panel d), the sidewalls morphologies, and the tilting features as well as uneven height characteristics of some nanowires in the arrays.

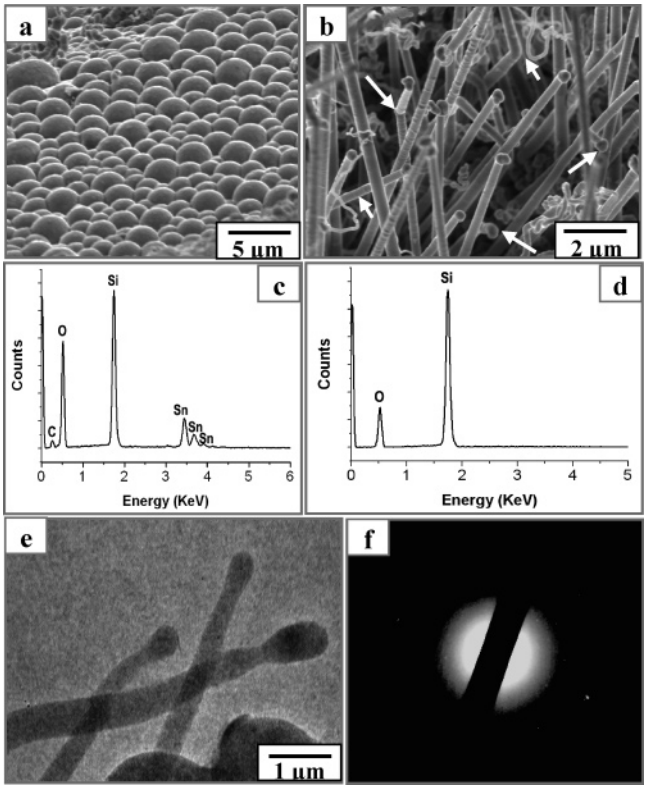

Figure 2. Electron microscopy characterization and composition analysis results: (a) SEM image of the large-scale alloyed balls emerging out of the surface of silicon substrate vigorously after 10 min of growth; (b) SEM image of the obtained nanowire arrays from the sample in panel a with additional 20 min growth, revealing that some nanowires possess a sharp-bending feature as indicated with arrows; (c, d) EDX analysis corresponding to panels a and b, respectively; (e) TEM image of the as-grown SiO_2 nanowires; and (f) SAED pattern of the nanowires, indicating the amorphous nature of the SiO_2 nanowires.

are cross-section SEM images of our SiO_2 nanowire arrays, revealing that large-scale, free-standing nanowires were grown nearly vertically and robustly in this region on the silicon substrate, and the nanowires have a typical length up to several tens of micrometers and a diameter in the range of 500 to 650 nanometers. To further analyze the morphology characteristic of the nanowires, high-magnification SEM images are presented in Figure 1c,d, confirming that most of the nanowires in the as-grown high-density products are free-standing on the substrate surface. Meanwhile, it is interesting to note that most nanowires show a slightly measurable tapering feature, with their average diameter varying from ca. 500 nm at the base and ca. 470 nm at the tip. Also, it is obvious that the surface of the nanowires in the array demonstrates a somewhat rough, undulating sidewalls profile, suggesting the occurrence of a concomitant CVD growth on the sidewalls of the nanowires during our fabrication.[29] Even though the close-up view of the wires (Figure 1c) indicates that there are many alloyed particles attached to the tip of the nanowires, which corresponds to the typical morphology of VLS-grown nanowires, we can clearly observe that the characteristic morphologies of some alloyed particles on the nanowires' tip are distinct, to some extent, from the commonly considered spherical shapes (indicated by arrows in Figure 1c,d). It should be pointed out that even though most of the nanowires in the array grow nearly vertically on the substrate, we can also observe that an appropriate portion of nanowires tilt obviously on the substrate (Figure 1b,c) and some nanowires show a different height in the array (Figure 1d). These

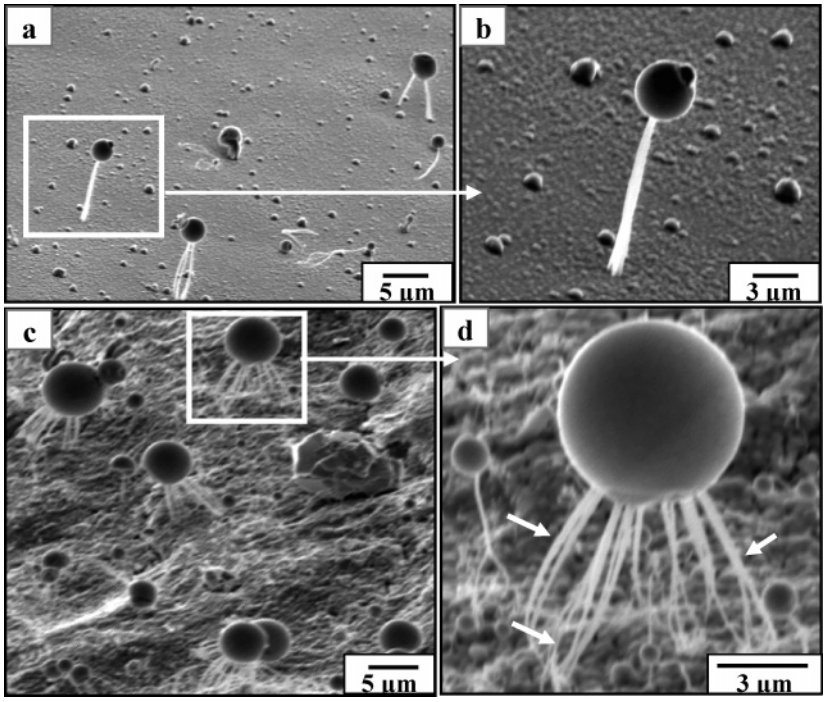

Figure 3. SEM images taken at different intermediate growth scenarios in a controlled experiment, revealing the novel growth styles of SiO_2 nanowires under the designed stable experimental condition: (a) the micrometer-sized bigger alloyed ball can simultaneously direct a number of nanowires' upward growth rather vertically (after 15 min reaction); (b) enlarged image of the boxed area indicated in panel a; (c) a growth scenario after 20 min of reaction revealing the striking up-lifting movements of the bigger alloyed rounded balls attached on different numbers of nanowires, while relatively smaller ones continuously come forth with the same growth style; (d) high-magnification image taken at the boxed area shown in panel c.

observations imply that a distinguishable growth style associated with the VLS-growth might occur in our protocol.

To better understand how the arrays of oriented silicon oxide nanowires were formed, we performed a series of time-dependent experiments to study the growth kinetics by FE-SEM. As shown in Figure 2a, at the early stage of nanowire growth (10 min of reaction), spectacular numbers of spherulitic nodules that are almost spherical in shape (with diameter in the range of 2 to 5 μm) emerge out robustly on the surface of silicon substrate.

The chemical composition of these spherical nodules can be judged from the energy-disperse X-ray spectroscopy (EDS) analysis (shown in Figure 2c), indicating that they are composed of Sn, Si, and O, along with trace of C. The sample shown in Figure 2a was then relocated in the reaction chamber to resume the growth process with an additional 20 min reaction. Quite interestingly, the obtained oriented nanowire arrays (Figure 2b) preserve the high-density, aligned features, consistent with those results shown in Figure 1. EDX analysis indicated that the nanowires are composed of Si and O with O/Si atomic ratios of $\sim$2.0 (Figure 2d). It is also striking to note that a number of ca. 500 nm diameter nanowires are highly flexible and can bend dramatically without breaking off near the nanowires' growth fronts (Marked with white arrows in Figure 2b), indicating that theses wires have an excellent mechanical property.[30] The transmission electron microscopy (TEM) image in Figure 2e presents the morphological characteristics of the as-synthesized silicon oxide nanowires scratched from the silicon substrate, exhibiting the alloyed-particle tips and the slightly tapering features. Electronic diffraction (ED) analysis of the obtained nanowires reveals that the SiO_2 nanowires are composed of amorphous SiO_2.

As we know, in a typical VLS growth, one catalyst particle usually catalyzes growth of just one nanowire. In our case, the formation of large-scale and remarkable micrometer-sized alloyed balls in the initial growth stage prompted us to discover what would take place next regarding these relatively big spherical alloyed particles. Namely, in what way can each of these catalyst particles stimulate the growth of SiO_2 nanowires and eventually lead to formation of the high-density, oriented nanowire arrays in our protocol?

To shed light on the subsequent formation process after the appearance of these nuclei sites−micrometer-sized balls, we have successfully controlled the number of the nuclei sites on the Si wafer by means of adjusting the source material while keeping other experimental parameters remain unchanged. After a 15 min reaction, the collected sample was subjected to FE-SEM investigation. Figure 3a represents an overview of the remarkable intermediate formation scenario. Astonishingly, one can see that several rounded alloyed balls attached onto the growth fronts of different numbers of SiO_2 nanowires have already sprung upward vigorously from the Si wafer surface while numbers of near-spherical alloyed nodules are formed in a style similar with that shown in Figure 2a. Specifically, a closed view in Figure 3b clearly reveals the striking up-lifting movement of the large alloyed ball, in which 3−4 pieces of individual SiO_2 nanowires grow out perpendicularly from the surface of the rounded bigger alloyed balls' lower hemisphere. Consequently, these derived nanowires made a corporative effort to tenaciously lift the micrometer-sized alloyed ball upward rather vertically in a very fascinating way under the current designed reaction condition. The sample with 20 min treatment in the controlled experiment gives us further information regarding the unique growth style. As shown in Figure 3c,d, some larger rounded alloyed balls with dimensions up to ca. 5−6 μm are lifting upward by several tens of nanowires. Meanwhile, many relatively small alloyed balls are continuously coming forth robustly with the same style as the bigger balls,

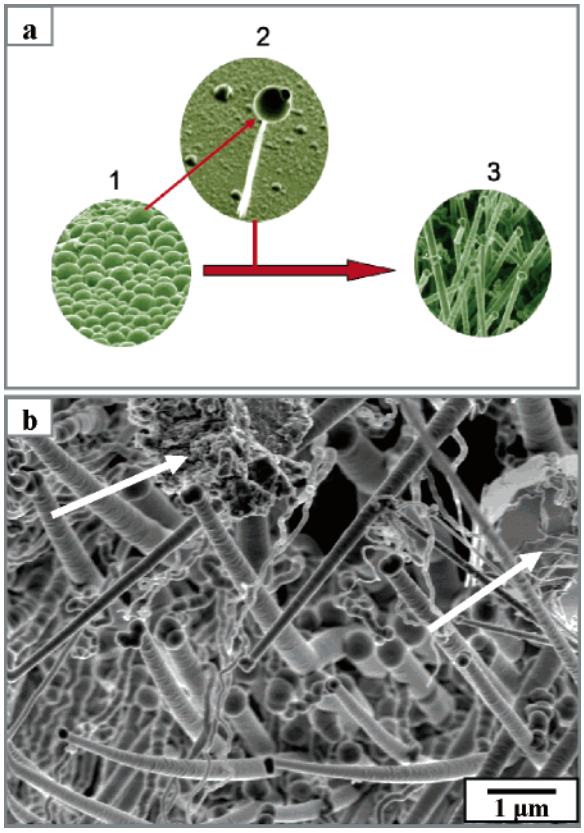

Figure 4. (a) Proposed growth steps for the synthesis of high-density, free-standing silicon oxide nanowire arrays under a specific designed reaction system: 1, pattern of micrometer-sized alloyed balls; 2, each alloyed ball has a lovely and fascinating up-lifting growth style; 3, eventual formation of nanowire arrays due to the impingement effect together with the designed local balanced and steady-state vapor environment in the double-tube reaction system. (b) SEM image of a sample with 25 min treatment, showing the broken alloyed ball and the debris attached on the tip of some nanowire (indicated with white arrows).

though not occurring at the same time. Clearly, the results suggest that the catalyst particle (micrometer-sized alloyed ball) moves upward with the growing nanowires, following the tip-growth prescription of the VLS growth.[27] Importantly, the present unusual growth styles undoubtedly indicate that each big micrometer-sized alloyed ball can simultaneously catalyze the growth of several to several tens of nanowires, which is quite different from the conventional VLS processes.

On the basis of the above-mentioned results, the following three consecutive growth steps are proposed for the synthesis of high-density, aligned SiO_2 nanowire arrays (as pictured in Figure 4a). First, the controlled deposition of Sn on the Si substrate leads to the large-scale pattern of Si−Sn alloyed balls. An explanation for this is that the Sn nanocluster, generated from the thermal evaporation of our source material, began to deposit onto the surface of the silicon wafer and grew into liquid Sn droplets.[31] Meanwhile, with an increasing amount of Si, vapor resulted from the thermal evaporation of Si wafers followed by condensation and dissolution, giving rise to the large-scale, remarkable micrometer-sized alloy droplet pattern (Figure 2a). Second, under the stable and balanced double-tube reaction system, the lower hemisphere of the obtained super-saturated micrometer-sized alloyed balls serves as preferential nuclei sites[20] for subsequent SiO_2 outward growth accompanied by a striking up-lifting movement (Figure 3), which demonstrates a rather unusual growth style, namely, each micrometer-sized alloyed ball can simultaneously catalyze the growth of several to several tens of nanowires. Third, the nanowires tenaciously increase in height during the extended reactions, until, above a certain critical height, the alloyed balls break down away (as shown in the Figure 4b), leading to the emergence of the two aforementioned characteristics of nanowires in the arrays. Namely, the debris originating from the broken-up ball will stay on the tips of the previous attached nanowires with an irregular morphology and uneven dimension. But the resulting debris attached on the tips of the nanowires can still direct the nanowires growth with the prolonged reaction to a different extent, thus giving rise to the nanowires in the array with somewhat different lengths together with irregular tip shapes (shown in Figure 1c,d). Also, some coarser or heavier debris might cause the corresponding nanowires to bend sharply, which is likely to account for the formation of sharp bending structures (indicated with arrows in Figure 2b). Additionally, after the breakup of the bigger alloyed ball, the peripheral nanowires (indicated with arrows in Figure 3d) in the wires bunch originating from the lower hemisphere of the alloyed ball will reasonably incline to some directions, therefore satisfactorily explaining the aforementioned tilting phenomenon observed in Figure 1b,c. Indeed, in our case, the VLS mechanism is responsible for the elongation of the nanowires, while a simultaneous gas-phase process piles up SiO_2 on the side of the growing wires,[29,32] hence resulting in the up-to-500 nm diameter free-standing nanowires with slightly tapering characteristics as well as somewhat rough sidewalls features. It should be emphasized that the designed local balanced and steady-state vapor environment guaranteed by the double-tube reaction system,[28] the initially synchronous formation of large-scale big micrometer-sized alloyed balls on the substrate, and the impingement effect[12,33] between the neighboring nanowires during the up-lifting growth stages are critical factors for the formation of the desired high-density, aligned nanowire arrays. Indeed, in a contrast experiment using a one-tube reaction system with the same parameters (reaction temperature, reaction duration, flow gas rate, etc.) as the double-tube reaction system, only sparsely populated, randomly oriented SiO_2 nanowires (Figure 5a) were produced.

The optical properties of the as-prepared SiO_2 nanowire arrays were investigated at room temperature. Figure 5b shows the photoluminescence (PL) spectrum with an excitation wavelength of 250 nm. The striking emission spectrum reveals that the as-synthesized SiO_2 nanowire array has a strong ultraviolet emission band centered at 385 nm (3.22 eV) and a relatively weaker ultraviolet emission one at 298 nm (4.16 eV). The 4.16 eV ultraviolet emission peak can be ascribed to originate from the existence of the two-fold-coordinated silicon lone-pair centers (≡O−Si−O≡), which correspond to some intrinsic diamagnetic defect centers.[34,35] The 3.22 eV band may be correlated with the formation of the ≡Si−O−C originating from the reaction between Si−O defects and carbon atoms during the nanowires' growth. Considering the source materials used in our protocol, it is possible to form carbon-doped silica in the present nanowire arrays.[36,37] According to previous research, the ultraviolet luminescence characteristics might have strong correlation with the collective behaviors of the obtained nanowire arrays.[38] Investigations are underway to elucidate the true nature of the observed optical behavior further. Nevertheless, the PL feature of the SiO_2 nanowire arrays is very stable; therefore, the resulting novel ultraviolet emission SiO_2 nanowire arrays are envisioned to be potentially used as promising UV laser emitters.

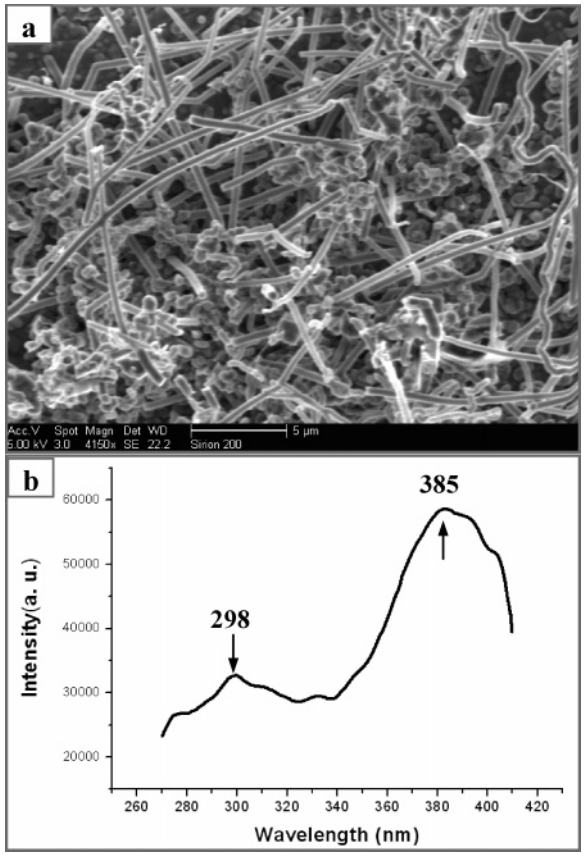

Figure 5. (a) For comparison, randomly distributed SiO_2 nanowires on the Si substrate synthesized from a reaction without the local balanced and steady ambient; (b) the PL spectrum of the as-synthesized high-density, aligned SiO_2 nanowire arrays.

4. Conclusions

In summary, high-density, well-aligned SiO_2 nanowire arrays were successfully fabricated by a simple designed chemical vapor deposition method that can guarantee a local balanced and steady-state reaction vapor environment. Surprisingly, direct observation of temporal evolution of the SiO_2 nanowire growth process via a microscopic imaging approach offers us amazing pictures related to the unique VLS growth styles: Initially, a large number of micrometer-sized alloyed ball patterns form in a large area, and then each of the alloyed balls cause the simultaneous growth of several to several tens of individual straight silica nanowires; finally the oriented silica nanowire arrays form under the designed experimental condition. These novel results are beneficial to understanding the formation mechanism of silica nanowire arrays, and at the same time, they extend our knowledge of VLS growth phenomena. The present results will definitely be helpful in nanostructure synthesis, ensuring the controlled growth of high-density, well-oriented functional nanowire arrays with desired morphologies. Moreover, the stable and strong ultraviolet emission properties of the as-grown products are of significant interest for their potential nanoscale optoelectronic device applications including ultraviolet-light-emitting devices, etc.

Acknowledgment. This work was financially supported by the Ministry of Science and Technology of China (Grant No. 2005CB623603) and the Natural Science Foundation of China (Grant No. 90406008). We thank Prof. C. M. Mo for valuable discussion.

References and Notes

(1) Cui, Y.; Lieber, C. M. *Science* **2001**, *291*, 851.
(2) Lee, S. T.; Wang, N.; Lee, C. S. *Mater. Sci. Eng. A* **2000**, *286*, 16.
(3) Xia, Y. N.; Yang, P. D.; Sun, Y.; Wu, Y. Y.; Mayers, B.; Gates, B.; Yin, Y.; Kim, F.; Yan, Y. *Adv. Mater.* **2003**, *15*, 353.
(4) Patzke, G.. R.; Krumeich, F.; Nesper, R. *Angew. Chem., Int. Ed.* **2002**, *41*, 2446.
(5) Rao, C. N. R.; Deepak, F. L.; Gundiah, G.; Govindaraj, A. *Prog. Solid. State Chem.* **2003**, *31*, 5−147.
(6) Zhang, R. Q.; Lifshitz, Y.; Lee, S. T. *Adv. Mater.* **2003**, *15*, 635.
(7) Rao, C. N. R.; Nath, M. *Dalton Trans.* **2003**, 1−25.
(8) Tenne, R.; Zettle, A. K. *Top. Appl. Phys.* **2001**, *80*, 81.
(9) Tenne, R. Angew. *Chem. Int. Ed.* **2003**, *42*, 5124.
(10) Xiao, Z. D.; Zhang, L. D.; Tian, X. K.; Fang, X. S. *Nanotechnology* **2005**, *16*, 2647.
(11) Ajayan, P. M.; Nugent, J. M.; Siegel, R. W.; Wei, B.; Kohler-Redlich, Ph. *Nature* **2000**, *404*, 243.
(12) Nerushev, O. A.; Dittmar, S.; Morjan, R. E.; Rohmund, E.; Campell, E. E. B. *J. Appl. Phys.* **2003**, *93*, 4185.
(13) Polleux, J.; Pinna, N.; Antonietti, M.; Niederberger, M. *J. Am. Chem. Soc.* **2005**, *127*, 15595
(14) Polleux, J.; Gurlo, A.; Barsan, N.; Weimar, U.; Antonietti, M.; Niederberger, M. *Angew. Chem., Int. Ed.* **2006**, *45*, 261.
(15) Pan, W. Z.; Dai, Z. R.; Wang, Z. L. *Science* **2001**, *291*, 1947.
(16) Zhou, J.; Gong, L.; Deng, S. Z.; Chen, J.; She, J. C.; Xu, N. S.; Yang, R. S.; Wang, Z. L. *Appl. Phys. Lett.* **2005**, *87*, 223108.
(17) Zygmunt, J.; Krumeich, F.; Nesper, R. *Adv. Mater.* **2003**, *15*, 1538.
(18) Jang, J.; Yoon, H. *Adv. Mater.* **2004**, *16*, 799.
(19) Kovtyukhova, N. I.; Mallouk, T. E.; Mayer, T. S. *Adv. Mater.* **2003**, *15*, 780.
(20) Zheng, B.; Wu, Y. Y.; Yang, P. D.; Liu, J. *Adv. Mater.* **2002**, *14*, 122.
(21) Zhu, Y. Q.; Hu, W. B.; Hsu, W. H.; Terrones, M.; Grobert, N.; Karali, T.; Hare, J. P.; Townsend, P. D.; Kroto, H. W.; Walton, D. R. M. *Adv. Mater.* **1999**, *11*, 844.
(22) Sun, S. H.; Meng, G. W.; Zhang, M. G.; Hao, Y. F.; Zhang, X. R.; Zhang, L. D. *J. Phys. Chem. B* **2003**, *107*, 13029.
(23) Pan, Z. W.; Dai, Z. R.; Ma, C.; Wang, Z. L. *J. Am. Chem. Soc.* **2002**, *124*, 1717.
(24) Yu, D. P.; Hang, Q. L.; Ding, Y.; Zhang, H. Z.; Bai, Z. G.; Wang, J. J.; Zou, Y. H. *Appl. Phys. Lett.* **1998**, *73*, 3076.
(25) Huang, M. H.; Mao, S.; Feick, H.; Yan, H. Q.; Wu, Y. Y.; Kind, H.; Weber, E.; Russo, R.; Yang, P. D. *Science* **2001**, *292*, 1987.
(26) Wagner, R. S.; Ellis, W. C. *Appl. Phys. Lett.* **1964**, *4*, 89.
(27) Ajayan, P. M. *Nature* **2004**, *427*, 402.
(28) Geng, C.; Jiang, Y.; Yao, Y.; Meng, X.; Zapien, J. A.; Lee, C. S.; Lifshitz, Y.; Lee, S. T. *Adv. Funct. Mater.* **2004**, *14*, 589.
(29) Hannon, J. B.; Kodambaka, S.; Ross, F. M.; Tromp, R. M. *Ntaure* **2006**, *440*, 69.
(30) Tong, L.; Gattass, R. R.; Ashcom, J. B.; He, S.; Lou, J.; Shen, M.; Maxwell, I.; Mazur, E. *Nature* **2003**, *426*, 816.
(31) Ye, C. H.; Zhang, L. D.; Fang, X. S.; Wang, Y. H.; Yan, P.; Zhao, J. W. *Adv. Mater.* **2004**, *16*, 1019.
(32) Liu, X.; Li, C.; Song, H.; Han, J.; Zhou, C. *Appl. Phys. Lett.* **2003**, *82*, 1950.
(33) Tian, Z. R.; Voigt, J. A.; Liu, J.; Mckerizie, B.; Mcdermott, M. J.; Rodriguez, M. A.; Konishi, H.; Xu, H. F. *Nature Mater.* **2003**, *2*, 821.
(34) An, X. H.; Meng, G. W.; Wei, Q.; Zhang, X. R.; Hao, Y. F.; Zhang, L. D. *Adv. Mater.* **2005**, *17*, 1781.
(35) Nishikawa, H.; Watanabe, E.; Ito, D.; Ohki, Y. *Phys. Rev. Lett.* **1994**, *72*, 2101.
(36) Hu, M. S.; Chen, H. L.; Shen, C. H.; Hong, L. S.; Huang, B. R.; Chen, K. H.; Chen, L. C. *Nature Mater.* **2006**, *5*, 102.
(37) Zhao, J.; Mao, D. S.; Lin, Z. X.; Jiang, B. Y.; Yu, Y. H.; Liu, X. H.; Wang, H. Z.; Yang, G. Q. *Appl. Phys. Lett.* **1998**, *73*, 1838.
(38) Yan, H. Q.; He, R. R.; Johnson, J.; Law, M.; Saykally, R. T.; Yang, P. D. *J. Am. Chem. Soc.* **2003**, *125*, 4728.